not known. The subbottom profile data show that the most recently deposited Holocene sediments are truncated by the crater (Fig. 3A). There is no evidence of a recent sediment drape over the deposits (Figs. 2 and 3B). The crater rim, internal walls, and debris field appear fresh (Fig. 2). Erosion or smoothing by bottom currents is not apparent. Together, the evidence suggests that the crater formed recently, probably within a few hundred years. An unusual sea-surface disturbance (possibly gas venting) was observed in the same vicinity in September 1906, but it is not possible to link this event with formation of the crater (*16*).

Hydrocarbon seepage is a relatively common process in the Gulf of Mexico, accounting for various phenomena such as gas-rich sediments hydrates, mud diapirs, and water column anomalies (*9, 10, 17, 18*). Release is usually gradual, but may be persistent (*18*). One example of natural high-energy venting was reported in 1200-m water depth (*16*). Also, a crater (about 40 m deep, 500 m in diameter) was tentatively recognized from a single acoustic profile in a water depth of 900 m (*19*). The high-resolution, deep-tow data now indicate that blowout-type craters and ejecta fields can form naturally in deep water following intrusive deformation of the sea floor.

REFERENCES AND NOTES

1. D. Prior *et al.*, *Science* **237**, 1330 (1987).
2. D. Prior and J. Coleman, in *Marine Slides and Other Mass Movements*, S. Saxov and J. Nieuwenhuis, Eds. (Plenum, New York, 1982), pp. 21–49.
3. K. Karlsrud and L. Edgers, in *ibid.*, pp. 61–68.
4. C. Hollister and N. McCave, *Nature* **309**, 220 (1984).
5. R. Martin and A. Bouma, *Mar. Geotech.* **5**, 63 (1982).
6. D. Prior *et al.*, *Proceedings of the Twentieth Offshore Technology Conference, OTC 5758,* 2 to 5 May 1988 (OTC, Houston, TX, 1988).
7. S. Miller, in *Natural Gases in Marine Sediments*, I. Kaplan, Ed. (Plenum, New York, 1974), pp. 151–177.
8. K. Campbell, J. Hooper, D. Prior, *Proceedings of the Eighteenth Offshore Technology Conference, OTC 5105,* 5 to 8 May 1986 (OTC, Houston, TX, 1986).
9. T. W. Neurater, thesis, Texas A&M University, 1988.
10. J. W. Brooks and W. Bryant, *Geological and Geochemical Implications of Gas Hydrates in the Gulf of Mexico* (Department of Energy, Morgantown, PA, 1985).
11. L. Roemer and W. Bryant, *Texas A&M Tech. Rep. 77-4-T* (1977).
12. T. Ferebee and W. Bryant, *ibid. 79-4-T* (1979).
13. J. Mackay, *Can. J. Earth Sci.* **24**, 1108 (1987).
14. W. Bryant and L. Roemer, in *Handbook of Geophysical Exploration at Sea*, R. Geyer, Ed. (CRC Press, Boca Raton, FL, 1983), pp. 123–186.
15. R. McQuillin *et al.*, *Inst. Geol. Sci. Rep. 90* (1979).
16. J. Soley, *Sci. Am. Suppl.* **1788**, 229 (1910).
17. B. Bernard *et al.*, *Earth Planet. Sci. Lett.* **31**, 48 (1976).
18. W. Sweet, *Am. Assoc. Petrol. Geol. Bull.* **58**, 1133 (1974).
19. T. Ferebee, Jr., thesis, Texas A&M University (1978).

20. We thank Shell Offshore Inc. for permission to use recently acquired data.

2 September 1988; accepted 28 November 1988

Rhenium-Osmium Isotope Systematics of Carbonaceous Chondrites

R. J. WALKER AND J. W. MORGAN

Rhenium and osmium concentrations and Os isotopic compositions of eight carbonaceous chondrites, one LL3 ordinary chondrite, and two iron meteorites were determined by resonance ionization mass spectrometry. Iron meteorite $^{187}Re/^{186}Os$ and $^{187}Os/^{186}Os$ ratios plot on the previously determined iron meteorite isochron, but most chondrite data plot 1 to 2 percent above this meteorite isochron. This suggests either that irons have significantly younger Re-Os closure ages than chondrites or that chondrites were formed from precursor materials with different chemical histories from the precursors of irons. Some samples of Semarkona (LL3) and Murray (C2M) meteorites plot 4 to 6 percent above the iron meteorite isochron, well above the field delineated by other chondrites. Murray may have lost Re by aqueous leaching during its preterrestrial history. Semarkona could have experienced a similar loss of Re, but only slight aqueous alteration is evident in the meteorite. Therefore, the isotopic composition of Semarkona could reflect assembly of isotopically heterogeneous components subsequent to 4.55 billion years ago or Os isotopic heterogeneities in the primordial solar nebula.

BECAUSE RE AND OS ARE HIGHLY refractory and siderophile elements, the Re-Os isotope system is particularly important in studies concerned with metal phases and high-temperature inclusions of meteorites. Potential applications of the system include dating meteorites, especially with respect to the chronology of the assembly and subsequent metamorphism of genetically disparate components, and providing estimates of the initial Os isotopic composition and Re/Os ratio of the early earth. This ratio is an important chemical tracer for understanding the formation of the earth's core and the chemical evolution of the mantle and crust. Because of analytical limitations, most Re-Os isotopic analyses of meteorites have been obtained from those metal phases that concentrated Re and Os (*1–3*). Data for IA, IIA, IIIA, and IVB iron meteorites define a line on a $^{187}Re/^{186}Os$ versus $^{187}Os/^{186}Os$ plot. Geochronologic applications, however, have been hindered by the lack of an accurate determination of the ^{187}Re half-life. Herr and co-workers (*3*) concluded that iron meteorites crystallized between 4 and 5 billion years ago (Ga) using a ^{187}Re half-life of $(4.3 \pm 0.5) \times 10^{10}$ years that was based on terrestrial molybdenite data (*4*). More recently, iron meteorites and metal separates from ordinary chondrites have been examined with secondary ion mass spectrometry (*1, 2*). A ^{187}Re half-life of $(4.56 \pm 0.12) \times 10^{10}$ years was derived with the assumption that chondrites and irons have a common age of 4.55 Ga. This result is within uncertainty of the half-life estimated from molybdenites and also of a value of $(4.36 \pm 0.13) \times 10^{10}$ years based on the laboratory determination of the growth of ^{187}Os in highly purified $HReO_4$ (*5*). Recent refinements of the laboratory determination, however, have yielded a half-life of $(4.23 \pm 0.13) \times 10^{10}$ years (*6*), which is significantly less than the meteorite-derived half-life.

We have measured the Re and Os concentration and Os isotopic composition for whole rock samples of eight carbonaceous chondrites and the unequilibrated LL3 ordinary chondrite Semarkona, as well as two iron meteorites. Chondrites represent one of the least distorted samples of the compositional and isotopic characteristics of the primordial solar nebula and thus provide information regarding the initial isotopic composition of Os in the early solar system.

We dissolved and equilibrated the samples (*7–9*) with enriched ^{190}Os and ^{185}Re spikes by alkaline fusion. Osmium was distilled twice as OsO_4 from H_2SO_4-H_2O_2 solution; Re was recovered from the residual solution by anion exchange. Both Re and Os were further purified by adsorption onto anion exchange beads and loaded onto a Ta filament. Total analytical blanks were <70 pg for Re and <20 pg for Os. Four Os isotopic ratios were measured with a resonance ionization mass spectrometer (*10*): ^{190}Os to ^{192}Os for determination of Os concentration by isotope dilution (ID); ^{192}Os to ^{188}Os for correction for mass fractionation, typically <1% per mass; and ^{192}Os to ^{187}Os and ^{188}Os to ^{187}Os for measurement of the relative abundance of ^{187}Os. These ratios were converted to $^{187}Os/^{186}Os$, the most commonly reported ratio, with $^{192}Os/^{186}Os$ and $^{188}Os/^{186}Os$ values of 25.59 and 8.302, re-

R. J. Walker, Department of Terrestrial Magnetism, Carnegie Institution of Washington, 5241 Broad Branch Road, NW, Washington, DC 20015.
J. W. Morgan, U.S. Geological Survey, Mail Stop 981, Reston, VA 22092.

spectively (*2*). Rhenium concentrations were determined by ID from $^{187}Re/^{185}Re$. Precisions (2σ) range from 0.8 to 2% for both concentration and isotope composition measurements. With the exception of Allende, which was provided as a powder, only unaltered interior pieces of meteorites were analyzed.

For interlaboratory comparison, we analyzed duplicate pieces of the Canyon Diablo (IA) and Tocopilla (IIA) iron meteorites (Table 1). These data plot within 2σ analytical uncertainties of the established iron meteorite isochron (*2*), indicating good interlaboratory agreement. A least-squares regression of these data and the iron meteorite data from Luck and Allègre (*2*) gives a slope of 0.06944 ± 0.00208 and an initial $^{187}Os/^{186}Os$ of 0.8119 ± 0.0094 (*11, 12*) (Fig. 1) (all regression uncertainties are 2σ). The absolute Re and Os concentrations agree less well with the literature values (*1–3*) (Table 1). The significant differences between replicate analyses of Canyon Diablo and Tocopilla likely reflect primary inhomogeneity at the 0.1- to 0.4-g sample size caused by coarse kamacite and taenite intergrowths.

Radiochemical neutron activation analysis (RNAA) data for Re and Os in carbonaceous chondrites show variation because of either analytical error or sample heterogeneity (*13–17*). Our ID data for the U.S. National Museum standard Allende powder (*18*) (Table 1) fall within the range of RNAA values, and the means agree well (2σ for the mean): 68.6 ± 3.5 ppb Re and 851 ± 62 ppb Os (ID; three determinations) versus 68.4 ± 5.2 ppb Re and 833 ± 65 ppb Os (RNAA; five determinations) (*15*). Variation in $^{187}Re/^{186}Os$ ranging from 3.00 ± 0.06 to 3.50 ± 0.10 indicates that Re and Os are mutually fractionated in important host phases. In Allende, a significant proportion of refractory metals occurs in calcium- and aluminum-rich inclusions as alloy grains of variable composition that may contain up to 46% Os and 4% Re (*19, 20*). A single osmium-rich alloy nugget only a few micrometers in diameter can increase substantially the concentration of Os in a 100-mg sample. Variations in concentrations were also observed in Murray (C2M) and Semarkona (LL3) when individual pieces were analyzed (Table 1). The nugget problem is less serious for these two meteorites and also the other carbonaceous chondrites of this study because calcium- and aluminum-rich inclusions are much rarer than in Allende and do not contribute significantly to refractory element abundances. Thus, these compositional heterogeneities are likely the result of analyzing pieces of these meteorites and not finely ground, mixed powders. The sporadic distribution of a relatively coarse metal phase might also account for the variations in the Semarkona data.

As a group, the carbonaceous chondrites have lower $^{187}Re/^{186}Os$ ratios (2.40 to 3.85) than the metal phases of ordinary chondrites (3.86 to 5.00) (*2*). The difference in Re/Os ratios between carbonaceous and ordinary chondrites (*14*) is not a result of fractionation between metal and silicate phases of the ordinary chondrites, because the Re/Os ratio by RNAA in whole-rock equilibrated chondrites agrees well with that determined by ID in separated metal phases (*21*). Semarkona, perhaps the least equilibrated ordinary chondrite, plots within the range of the carbonaceous chondrites. Among carbonaceous chondrites, the trend of increasing $^{187}Re/^{186}Os$ with increasing grade inferred from the RNAA data (*21*) is not apparent from the ID data. The lowest chondritic $^{187}Re/^{186}Os$ ratio is from Karoonda, a C4O chondrite.

All data for carbonaceous chondrites plot above the iron meteorite isochron, and all but three pieces of Murray plot systematically in a range 1 to 2% above the isochron. In addition, Luck and Allègre (*2*) reported that nine of ten of the separated metal phases of chondrites also plot above the isochron. The exception, Dhajala (H3.8) is an unequilibrated chondrite in which the metal may not be in chemical or isotopic equilibrium with other phases with respect to refractory siderophile elements (*22*). Although many of these chondrites plot within analytical uncertainty of the iron meteorite isochron, this offset indicates that there is a significant isotopic difference between irons and chondrites. For a sign test, the probability of 18 out of 19 chondrites plotting above the line, if both groups were derived from isotopically identical reservoirs at the same time, is 8×10^{-5}. Thus, if identical closure ages are assumed for both chondrites and irons, the initial $^{187}Os/^{186}Os$ of chondrites is 1 to 2% higher than that for irons. A least-squares fit of our carbonaceous chondrite data, except for Murray, to a line with a slope defined by a closure age of 4.55 Ga and with the most recent half-life value of 42.3 billion years gives an initial $^{187}Os/^{186}Os$ of 0.802 ± 0.049 (Fig. 2). When the data from metal separates of ordinary chondrites (*2*) are included in the regression, the intercept is 0.794 ± 0.024. Different initial isotopic compositions for meteorite groups of the same age would imply that the precursor materials had different multistage Re-Os histories before system closure. Alternatively, the differences between the Re-Os systematics of chondrites and irons may result from different closure ages. Other radiomet-

Table 1. Rhenium and Os abundances and Os isotopic ratios in iron meteorites, carbonaceous chondrites, and unequilibrated ordinary chondrite Semarkona (2σ errors).

Meteorite*	Type	Re (ppb)	Os (ppb)	$^{187}Re/^{186}Os$	$^{187}Os/^{186}Os$
			Irons		
Canyon Diablo	IA	247 ± 2	2620 ± 30	3.78 ± 0.06	1.07 ± 0.01
		272 ± 2	2930 ± 30	3.74 ± 0.06	1.08 ± 0.01
(*3*)†		252 ± 7	2070 ± 30	4.88 ± 0.15	1.13 ± 0.02
					1.12 ± 0.01
(*2*)		247 ± 2	2300 ± 40	4.33 ± 0.16	1.12 ± 0.01
		222 ± 4	2030 ± 40	4.40 ± 0.12	1.11 ± 0.01
Tocopilla	IIA	230 ± 2	1080 ± 10	8.56 ± 0.14	1.39 ± 0.02
		247 ± 4	1090 ± 10	9.16 ± 0.15	1.45 ± 0.01
(*3*)†		252 ± 5	1290 ± 70	7.87 ± 0.63	1.41 ± 0.01
					1.43 ± 0.01
(*2*)		222 ± 4	1060 ± 20	8.42 ± 0.30	1.40 ± 0.01
			Chondrites		
Orgueil	C1I	43.3 ± 0.9	518 ± 4	3.36 ± 0.10	1.07 ± 0.02
Murchison	C2M	56.3 ± 0.6	759 ± 8	2.98 ± 0.05	1.03 ± 0.01
Murray	C2M	53.2 ± 1.0	713 ± 3	3.00 ± 0.07	1.06 ± 0.01
		67.0 ± 0.7	810 ± 8	3.33 ± 0.05	1.09 ± 0.01
		66.6 ± 1.0	714 ± 7	3.74 ± 0.07	1.12 ± 0.01
		69.3 ± 0.6	750 ± 7	3.71 ± 0.05	1.09 ± 0.02
Ornans	C3O	67.5 ± 0.8	822 ± 7	3.30 ± 0.08	1.05 ± 0.01
Lancé	C3O	73.9 ± 1.0	919 ± 12	3.23 ± 0.06	1.04 ± 0.02
Allende	C3V	65.8 ± 1.3	819 ± 8	3.23 ± 0.06	1.05 ± 0.01
		68.1 ± 0.7	911 ± 9	3.00 ± 0.06	1.04 ± 0.01
		71.8 ± 2.0	824 ± 8	3.50 ± 0.10	1.07 ± 0.01
Vigarano	C3V	66.3 ± 0.8	795 ± 5	3.35 ± 0.04	1.06 ± 0.01
Karoonda	C4O	72.5 ± 0.7	1210 ± 14	2.40 ± 0.04	1.00 ± 0.01
Semarkona	LL3	47.6 ± 0.9	496 ± 6	3.85 ± 0.08	1.09 ± 0.01
		43.4 ± 0.6	536 ± 4	3.25 ± 0.05	1.10 ± 0.01

* Reference entries indicate data from other studies. † Rhenium and osmium abundances determined by neutron activation. Errors are 2σ derived from four determinations of 1- to 2-g samples.

ric isotope systems indicate that the primary crystallization age of chondrites is approximately 4.55 Ga. However, ages ranging from 4.55 to 3.8 Ga have been reported for different iron meteorites as determined by Ar, Sr, Xe, and Ag dating techniques (*23*). If the 42.3 billion year half-life for ^{187}Re is accepted, the Re-Os closure age of the iron meteorites of this study and (*2*) is 4.15 ± 0.16 Ga.

The Re-Os isotope data for three of four samples of Murray (C2M) plot 2 to 3% above the carbonaceous chondrite isochron (Fig. 3). The remaining sample has a less radiogenic composition that is consistent with the other chondrites, indicating that the meteorite is isotopically heterogeneous. Murray is unequilibrated and may have preserved primordial isotopic heterogeneities in some phases. No corresponding Nd or O isotopic anomalies have been reported, but the decay constant of ^{187}Re may be particularly sensitive to temperature and electron density in stellar interiors (*24*). The meteorite has undergone substantial preterrestrial aqueous alteration (*25*), and there is evidence of significant leaching (*26*). Hence, loss of Re at some time subsequent to 4.55 Ga, perhaps as the highly soluble perrhenate ion, alternatively may account for the apparent ^{187}Os excess. Comparable Rb-Sr and U-Th-Pb isotopic heterogeneities in chondrites have been attributed to disturbances that significantly postdate 4.55 Ga (*27*). Leaching of Re could have occurred either soon after the formation of the meteorite or could significantly postdate its formation. If leaching occurred soon after formation, however, the magnitude of the offsets would require rapid growth of the apparent excess ^{187}Os in a domain with a very high Re/Os ratio and subsequent removal of much of the Re by leaching.

Apparent excess ^{187}Os was also observed in one of the two samples of Semarkona (Fig. 3). This unequilibrated meteorite is also inhomogeneous with respect to other isotopes (*28*), most notably containing a phase with the highest deuterium content yet observed (*29*). Semarkona shows a degree of preterrestrial aqueous alteration that is unusual in ordinary chondrites (*30*). Variable $^{187}Os/^{186}Os$ could have been caused by leaching of Re in the same manner as discussed for Murray, although aqueous alteration is much less extensive in Semarkona than in Murray. The Os isotopic heterogeneities alternatively might have resulted from the assembly of phases with differing initial Os isotopic compositions at or postdating 4.55 Ga. If assembly postdated 4.55 Ga, then the components included materials that evolved with at least two stages of Re-Os evolution, one with a high Re/Os ratio. If the assembly occurred within several million years of the formation of the solar system, then the heterogeneities may indicate isotopic variability in the primordial solar nebula.

The Re-Os systematics of carbonaceous chondrites are thus similar, but probably not identical to those of iron meteorites. The apparent subtle differences may result from a more recent Re-Os closure age for irons, on the order of several hundred million years. Alternatively, the results might indicate that the precursors to these meteorite groups evolved with different, multistage Re-Os histories. The average Os isotope composition of these carbonaceous chondrites is consistent with age-normalized data for some terrestrial mantle-derived rocks, supporting the speculation that the earth's mantle has evolved with Re-Os systematics similar to those of carbonaceous chondrites (*31*). In addition, the large isotopic heterogeneities observed in Murray and Semarkona indicate that these meteorites either accumu-

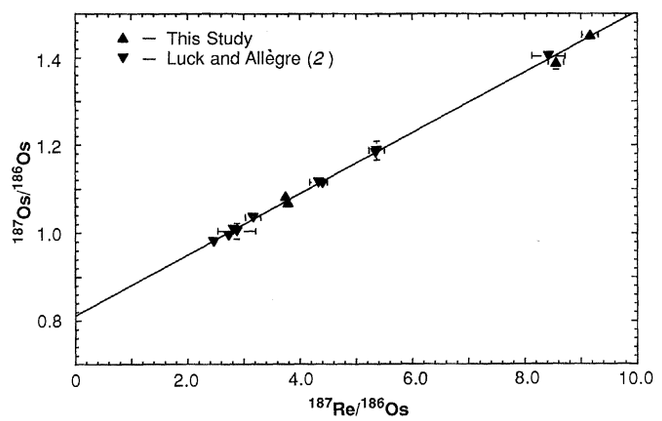

Fig. 1. $^{187}Re/^{186}Os$ versus $^{187}Os/^{186}Os$ diagram showing duplicate analyses of both Tocopilla and Canyon Diablo iron meteorites and the iron meteorite data reported by Luck and Allègre (*2*). Error bars are 2σ. All data plot within analytical uncertainty of an isochron defining a slope of 0.06944 ± 0.00208 and an initial $^{187}Os/^{186}Os$ ratio of 0.8119 ± 0.0094. The variation in Re/Os ratio between the two samples of Tocopilla probably reflects heterogeneities in the meteorite at the 0.1 to 0.4 g sample size.

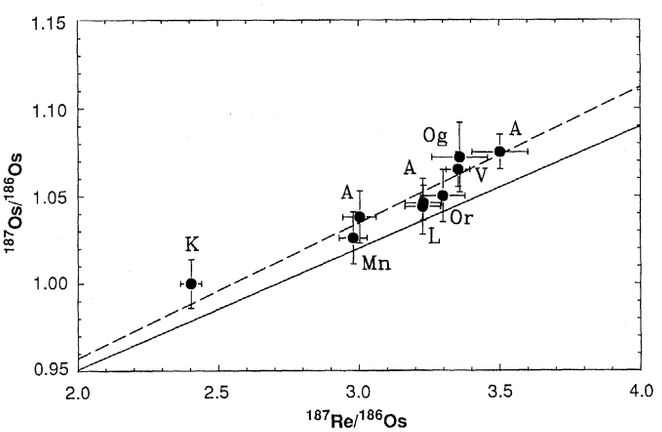

Fig. 2. $^{187}Re/^{186}Os$ versus $^{187}Os/^{186}Os$ diagram showing data for seven carbonaceous chondrites, including triplicate analyses for Allende. The iron meteorite isochron is shown as a solid line; the dashed line shows a least-squares fit of the carbonaceous chondrite data to a line with a slope defined by a 4.55 Ga age and a ^{187}Re half-life of 4.23×10^{10} years (slope = 0.07741). The initial $^{187}Os/^{186}Os$ ratio of this line is 0.802 ± 0.049. Abbreviations: A, Allende; K, Karoonda; L, Lance; Mn, Murchison; Og, Orgueil; Or, Ornans; and V, Vigarano.

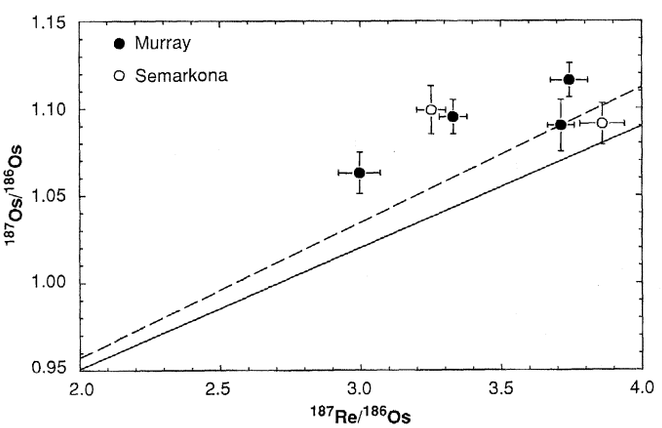

Fig. 3. $^{187}Re/^{186}Os$ versus $^{187}Os/^{186}Os$ diagram showing large offsets of several samples of Murray and Semarkona from the iron and carbonaceous chondrite isochrons. The data suggest that the meteorites are isotopically heterogeneous and the offsets may indicate either Re leaching during aqueous alteration or accumulation of isotopically heterogeneous parts.

lated from isotopically heterogeneous materials or that Re was leached at some stage following their accretion.

REFERENCES AND NOTES

1. J.-M. Luck *et al.*, *Nature* **283**, 256 (1980).
2. J.-M. Luck and C. J. Allègre, *ibid.* **302**, 130 (1983).
3. W. Herr, W. Hoffmeister, B. Hirt, J. Geiss, F. G. Houtermans, *Z. Naturforsch.* **16A**, 10, 1053 (1961).
4. B. Hirt *et al.*, *Radioactive Dating* (International Atomic Energy Agency, Vienna, 1963).
5. M. Lindner *et al.*, *Nature* **320**, 246 (1986).
6. M. Lindner *et al.*, *Univ. Calif. Res. Lab. Preprint 99534* (1988).
7. R. J. Walker and J. D. Fassett, *Anal. Chem.* **58**, 2923 (1986); J. D. Fassett and R. J. Walker, *Inst. Phys. Conf. Ser. No. 84*, 115 (1987).
8. J. D. Fassett, R. J. Walker, J. C. Travis, F. C. Ruegg, *Int. J. Mass Spectrom. Ion Proc.* **75**, 111 (1987).
9. J. W. Morgan and R. J. Walker, *Anal. Chim. Acta*, in press.
10. The resonance ionization mass spectrometer consisted of a 15-cm radius-of-curvature mass spectrometer coupled with a 10-Hz Nd-YAG–pumped tunable dye laser with frequency doubling. Wavelengths were tuned to selectively photoionize Os and Re from a gas-phase reservoir produced from a Ta filament. The detection system consisted of an electron multiplier interfaced with a transient digitizer.
11. J. H. Williamson, *Can. J. Phys.* **46**, 1845 (1968).
12. D. York, *Earth Planet. Sci. Lett.* **5**, 320 (1969).
13. J. W. Morgan and J. F. Lovering, *Geochim. Cosmochim. Acta* **37**, 1893 (1967).
14. E. Anders *et al.*, *ibid.* **40**, 1131 (1976).
15. H. Takahashi *et al.*, *ibid.* **42**, 97 (1978).
16. R. Wolf *et al.*, *ibid.* **44**, 711 (1980).
17. M. Ebihara *et al.*, *ibid.* **46**, 1849 (1981).
18. E. Jarosewich, R. S. Clarke, J. N. Barrows, Eds., The Allende Meteorite Reference Sample, *Smithsonian Contribution to the Earth Sciences no. 27* (Smithsonian Institution, Washington, DC, 1986).
19. A. Bischoff and H. Palme, *Geochim. Cosmochim. Acta* **51**, 2733 (1987).
20. J. T. Armstrong, I. D. Hutcheon, G. J. Wasserburg, *ibid.*, p. 3155.
21. J. W. Morgan, *Nature* **317**, 703 (1985).
22. C.-L. Chou, P. A. Baedecker, J. T. Wasson, *Geochim. Cosmochim. Acta* **37**, 2159 (1973).
23. D. S. Burnett and G. J. Wasserburg, *Earth Planet. Sci. Lett.* **2**, 137 (1967); H. G. Sanz, D. S. Burnett, G. J. Wasserburg, *Geochim. Cosmochim. Acta* **34**, 1227 (1970); S. Niemeyer, *ibid.* **44**, 33 (1980); T. Kaiser and G. J. Wasserburg, *ibid.* **47**, 43 (1983).
24. K. Takahashi and K. Yokoi, *Nucl. Phys.* **A404**, 578 (1983).
25. T. E. Bunch and S. Chang, *Geochim. Cosmochim. Acta* **44**, 1543 (1980).
26. G. W. Kallemeyn and J. T. Wasson, *ibid.* **45**, 1217 (1981).
27. D. W. Mittlefehldt and G. W. Wetherill, *ibid.* **43**, 201 (1979); J.-F. Minster, J.-L. Birck, C. J. Allègre, *Nature* **300**, 414 (1982); F. Tera, *Earth Planet. Sci. Lett.* **63**, 147 (1983).
28. J. N. Grossman, R. N. Clayton, T. K. Mayeda, *Meteoritics* **22**, 395 (1987); C. M. Alexander *et al.*, *Lunar and Planetary Science XIX*, 5 (1988); I. D. Hutcheon, R. Hutchinson, G. J. Wasserburg, *ibid.*, p. 523; T. D. Swindle, J. N. Grossman, D. H. Garrison, C. T. Olinger, *ibid.*, p. 1165.
29. N. J. McNaughton, A. E. Fallick, C. T. Pillinger, *J. Geophys. Res.* **87**, 297 (1982).
30. R. Hutchinson, C. M. O. Alexander, D. J. Barber, *Geochim. Cosmochim. Acta* **51**, 1875 (1987).
31. C. J. Allègre and J.-M. Luck, *Earth Planet. Sci. Lett.* **48**, 148 (1980).

32. We thank R. S. Clarke, E. Jarosewich, and G. MacPherson of the Smithsonian Institution, Washington, DC, and C. B. Moore of Arizona State University for meteorite samples. The Mass Spectrometry group of the National Institute of Standards and Technology is thanked for the use of the RIMS instrument.

9 September 1988; accepted 12 December 1988

The Effect of GTPase Activating Protein upon Ras Is Inhibited by Mitogenically Responsive Lipids

MEN-HWEI TSAI, CHUN-LI YU, FU-SHENG WEI, DENNIS W. STACEY

Bacterially synthesized c-Ha-*ras* protein (Ras) was incubated with guanosine triphosphatase (GTPase) activating (GA) protein in the presence of various phospholipids. The stimulation of Ras GTPase activity by GA protein was inhibited in some cases. Among the lipids most active in blocking GA protein activity were lipids that show altered metabolism during mitogenic stimulation. These included phosphatidic acid (containing arachidonic acid), phosphatidylinositol phosphates, and arachidonic acid. Other lipids, including phosphatidic acid with long, saturated side chains, diacylglycerols, and many other common phospholipids, were unable to alter GA protein activity. The interaction of lipids with GA protein might be important in the regulation of Ras activity during mitogenic stimulation.

CELLULAR *RAS* PROTEIN (RAS) appears to be critical during mitosis (*1*). Although it is not known how Ras functions, the regulation of Ras activity could be essential in the control of cellular proliferation (*2*). A cytoplasmic GTPase activating (GA) protein stimulates the rate at which Ras converts bound guanosine triphosphate (GTP) to guanosine diphosphate (GDP) (*3*). Since this conversion is believed to inactivate Ras, GA protein might be involved in negatively regulating Ras activity. On the other hand, studies with *ras* mutants suggest that Ras might control the activity of GA protein (*4, 5*). In either case, the interaction between these two proteins could be involved in the control of cellular proliferation, although it has not been shown that the interaction between Ras and GA protein can be modified during mitogenic stimulation. Microinjection of antibody to Ras, however, indicated that the mitogenic action of several lipid-related materials was dependent upon cellular Ras activity (*6*). It was postulated that phospholipid metabolism might be related to the biological activation of cellular Ras and therefore to the interaction between GA protein and Ras.

GTPase activating protein (often called GAP) activity has been identified in crude cytoplasmic extracts from a variety of cell types, it has been purified, and the gene has been cloned (*7, 8*). GA protein increases the GTPase activity of purified, bacterially synthesized Ras in solution or of cellular Ras associated with crude membrane preparations. We initially used crude mouse brain cytosol as our source of GA protein (*9*) and then also used bacterially synthesized, cellular Harvey Ras. In the first analysis, liposomes of phosphatidic acid with saturated fatty acid side chains (stearic acid) were

Department of Molecular Biology, The Cleveland Clinic Foundation, 9500 Euclid Avenue, Cleveland, OH 44106.

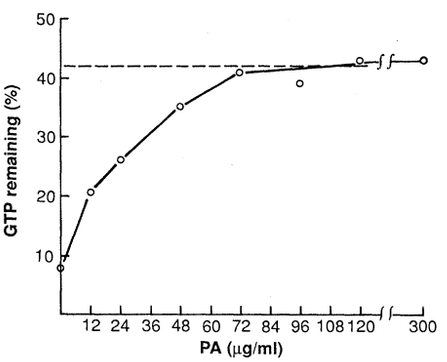

Fig. 1. Inhibition of GA protein activity by increasing concentrations of phosphatidic acid. (PA) Bacterially synthesized Ras was bound to [α-^{32}P]GTP and then incubated with crude GA protein in the presence of various concentrations of phosphatidic acid. After 1 hour, the Ras was precipitated with a specific antibody and the ratio of bound nucleotides was determined with TLC. The broken line indicates the percentage of GTP remaining bound to Ras in the absence of GA protein or phospholipid. The ability of GA protein to increase GTPase and decrease the amount of bound GTP was inhibited approximately 50% by 24 μg/ml phosphatidic acid. Nucleotide-free Ha-Ras (2 μ*M*) was incubated for 20 min at 30°C with 1 μ*M* [α-^{32}P]GTP (3000 Ci/mmol; Amersham) in 50 μl of tris-HCl, *p*H 7.5, buffer containing 2 m*M* dithiothreitol without added $MgCl_2$. GTPase reaction was initiated by addition of $MgCl_2$ and crude GA protein preparation (*3–5, 9*) and the indicated concentrations of phosphatidic acid (γ-stearoyl β-arachidonoyl) in 150 μl of reaction buffer [final concentrations: 20 m*M* tris-HCl, *p*H 7.5, 3 m*M* $MgCl_2$, 0.15*M* NaCl, 1 m*M* dithiothreitol (*23*)]. After incubation at 30°C for 1 hour, Ras was immunoprecipitated by monoclonal antibody Y13-259 and protein A–Sepharose beads coated with rabbit antibody to rat immunoglobulin G (*3, 4*). Bound nucleotides were released from the immunoprecipitate by boiling for 3 min. Bound nucleotides were resolved on a polyethyleneimine cellulose TLC plates (EM Science) in 1*M* potassium phosphate, *p*H 3.4, visualized by autoradiography and quantitated. Liposomes were formed as in (*12*). Ha-*ras* protein was prepared in a bacterial expression system as described (*24*).